Solid Freeform Fabrication 2019: Proceedings of the 30th Annual International Solid Freeform Fabrication Symposium – An Additive Manufacturing Conference
Reviewed Paper

IMPACT OF FLOW AID ON THE FLOWABILITY AND COALESCENCE OF POLYMER LASER SINTERING POWDER

R.G. Kleijnen*, M. Schmid*, and K. Wegener†

*inspire AG, Innovation Center for Additive Manufacturing Switzerland, Lerchenfeldstrasse 3, 9014 St. Gallen, Switzerland
†Swiss Federal Institute of Technology, ETH Zürich, Institute of Machine Tools and Manufacturing (IWF), Leonhardstrasse 21, 8092 Zurich, Switzerland

Abstract

Small amounts of nanometer-sized flow aids are typically added to polymer powders for selective laser sintering to increase flowability. These additives reduce friction between particles by electrostatic repulsion, leading to better bed density and part properties. The same repulsion however can hinder particle coalescence in the melt, reducing part density. This study investigates the effect of different amounts of flow aid on flowability and coalescence. A polybutylene terephthalate (PBT) powder with spherical morphology, specially designed for selective laser sintering, is used as a base and ideal model material. The coalescence is monitored by hot-stage optical microscopy. It was found that with increasing amounts of flow aid, the flowability could be characterized by three regions; one of low flowability where the powder contained insufficient flow aid, followed by a sharp transition region towards a high flowability region, where the flow aid was most effective. Addition of flow aid impacted the coalescence, which was marked by an increase of the temperature at which the particles started to melt and flow. At the maximum concentration of 0.5 wt.-% flow aid, the melting of some particles was delayed, and they remained solid for longer time at temperatures beyond the melting temperature. The optimum amount of flow aid therefore lies in the plateau region of high flowability, but before the occurrence of delayed melting.

Introduction

Selective Laser sintering (SLS) is a primary shaping process; the properties of parts depend on many material- and process-based factors. One of these is the flowability of the powder. A key step during the LS process is the deposition of a powder layer, which is typically between 80 and 120 µm thick. The flowability determines to what extent powder can be deposited in a layer, and how densely the powder particles are packed. The density of the powder layer is closely related to the density of produced parts, shown for example by Schmid et al. [1]. To obtain dense parts with optimal mechanical properties, the powder flowability must be optimized. The most widely applied method to improve powder flowability is to add a small amount of nanometer-sized flow aid, demonstrated amongst others in [2–7]. These flow aids are typically a variant of fumed silica and added in quantities between 0.01 % and 0.5 % by weight.

Flow aids work based on the principle of electrostatic and steric repulsion, explained in [8]. Without flow aid, polymer particles may cling together because of interparticle van-der-Waals forces, which is elaborated in detail by Rumpf [9]. The presence of flow aid increases the interparticle distance, thereby decreasing the adhesive forces between them. On a macroscopic scale, this improves powder flow. The right choice of flow aid is critically important. Blümel et al. [7] added 0.5 wt.-% of hydrophobic and hydrophilic flow aid to high density polyethylene (HDPE) powder. The powder flowability was measured with a shear cell

and by determination of the bulk density. They found that while the hydrophobic flow aid drastically increased the powder flow properties, the hydrophilic flow aid had no significant, or in the case of the bulk density, even detrimental effect. Most authors opted for hydrophobic flow aids and obtained their desired results. Lexow and Drummer [2] measured an increase of bulk density of a cryogenically ground polypropylene (PP) powder upon addition of 0.1 wt.-% Aerosil® 8200. The influence of varying amounts of Aerosil® R106 on the flowability of cryomilled HDPE and PP powders, expressed amongst others by the Hausner ratio, was investigated by Laumer et al. [3]. They found an optimal flowability for HDPE at 0.25 wt.-% flow aid concentration. Addition of more flow aid was less effective. This was attributed to saturation of the particle surface, and subsequent agglomeration of the flow aid itself. The same effect was not observed for the PP powder; a continuous increase of powder flowability up to concentrations of 1.0 wt.-% flow aid was reported. To improve the flowability of a cryogenically ground PBT copolymer powder, Arai et al. [4] added 0.1 wt.-% Aerosil® R200H. They observed enhanced flowability, and were able to determine that the flow aid did not have any effect on the thermal properties of the material.

To achieve high density laser sintered parts, not only the flow behavior of the powder is important, but also the rheology and surface tension of the polymer in the melt, which is described by Schmid [10]. Fumed silica's are also used as additives to influence rheology, and to create materials with thixotropic behavior. Even though the flow aid concentration in SLS materials is relatively low compared to the concentration used to influence rheology, it is imaginable that particle coalescence in the melt can be affected by the flow aid presence. Benedetti et al. summarized the usability of various evaluation methods based on different optical features of particles in hot-stage optical microscopy (HS-OM) [11]. The coalescence of polymer SLS powders has been investigated by various other researchers. The coalescence rate of three polyether(ether)ketone (PE(E)K) powders with different viscosities was determined by Berretta et al. [12], by tracking the neck formation with HS-OM. Particle coalescence was slower for the grades with higher viscosities, but the interpretation of the results is difficult due to the irregular shape of the cryomilled particles. Verbelen et al. [13] tracked the coalescence of different commercial polyamide-based SLS powders with HS-OM. In a later study, Dadbakhsh et al. [14] used HS-OM to view the coalescence of polyamide-12 powders at different degrees of aging. They identified a slow softening region up to the onset melting temperature of the polymer, followed by a fast coalescence and a subsequent molten phase region. Coalescence occurred slower for powders that had aged more, which was attributed to the increased molecular weight and associated melt viscosity due to the aging. Hejmady et al. [15] used a special setup to observe the coalescence of two laser sintering particles as they are molten by laser irradiation, providing further insight to the melting and coalescence behavior of particles during the actual laser sintering process.

HS-OM has been identified as a method to both qualitatively and quantitatively assess the coalescence of polymer powders. It is used in this work to assess the effect of different amounts of flow aid on particle coalescence of a spherical polybutylene terephthalate (PBT) powder. Complemented with determination of the powder flowability as expressed by the Hausner ratio, as well as the avalanche angle and avalanche fractal from powder rotational measurements, the optimal concentration can be determined. Comparable results are, according to the authors' knowledge, not available in present literature.

Materials and Methods

Materials. PBT TORAYCON 1200M (TORAY, Tokyo, Japan) was obtained in granulate form. The material did not contain any stabilizers or other additives to prevent these from affecting the SLS process. Hydrophobic fumed silica Aerosil® R812 flow aid (Evonik Ind., Essen, Germany) was obtained and used without further modification. Aerosil R812 is a trimethyl terminated fumed silica, and considered a good general choice for improving the flowability of different polymer powders.

Powder Production. The PBT powder was produced via melt emulsification. During this process, the target material is melt blended in a single-screw extruder with a water-soluble resin. The production of the particular powder used in this study is extensively described in [16]

Material preparation. The PBT powder was dry blended with R812 flow aid in a rotating mixing drum with a diameter of 200 mm. The drum shown in figures 1 and 2, was specially designed to facilitate mixing of two components. Each blend was mixed for 30 minutes with a rotation speed of 60 rpm. First, a masterbatch containing 0.5 wt.-% of flow aid was prepared. This masterbatch was used to prepare the blends listed in table 1. The weight of each blend totaled 100 g.

Table 1. Prepared blends of PBT and flow aid.

Designation	Flow aid concentration [wt.-%]	Comment
PBT_0.5	0.5	Masterbatch
PBT_0.1	0.1	
PBT_0.05	0.05	
PBT_0.01	0.01	
PBT_0.005	0.005	
PBT_Virgin	0.0	No flow aid

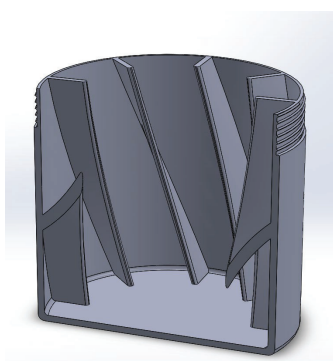

Figure 1. Schematic cross-section of the used mixing drum

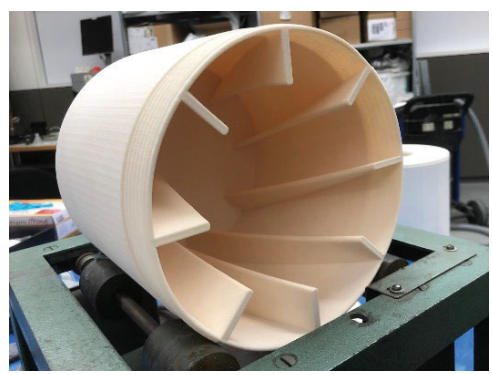

Figure 2. Mixing drum on mixing stage (shown here without lid)

Particle size distribution. The particle size distribution was measured by dynamic light scattering on an LS230 (Beckman Coulter, Brea, CA, United States) instrument. Approximately 0.1 g of powder was added to approximately 20 ml acetone and thoroughly stirred. The particle size was calculated based on the Fraunhofer diffraction model, for the range between 0.4–2000 µm.

Scanning electron microscopy. Scanning electron microscopy images were obtained on a JSM 7100F scanning electron microscope (JEOL, Tokyo, Japan). Samples were deposited on a piece of carbon tape on an aluminium SEM stub and sputter coated with a 10 nm layer of Pt/Pd (80/20).

Thermal analysis. Differential Scanning Calorimetry (DSC) measurements were carried out on a DSC 25 (TA Instruments, New Castle, DE, United States). All measurements were conducted under a nitrogen atmosphere, from 25°C to 250°C, with heating and cooling rates of 10°C/min.

Powder flowability. The powder flowability as expressed by the Hausner ratio was determined by measurement of the powder bulk and tapped density. The bulk density was determined by filling a 25 ml brass cup with powder through a Carney funnel and recording the weight. Each powder blend was measured three times. The tapped density was determined with a BeDensiT3 Tap Density Volumeter (Dandong Bettersize Instruments, Liaoning, China). One measurement consisted of filling three measuring cylinders with 25 g of powder each. The cylinders were then automatically tapped 1'500 times with a frequency of two taps per second. The powder volume at the end of the tapping cycle divided by its weight gives the powder tapped density.

The powder flowability was also evaluated with a Revolution Powder Analyzer (RPA) (Mercury Scientific, Newtown, CT, United States). An exact measure of 25 mL, respectively 21.8 g powder at tapped density was added to a drum with a diameter of 50 mm. The drum was rotated with a speed of 0.6 rpm, while a camera recorded 384 avalanche events. Each time directly following an avalanche, the avalanche angle and roughness of the powder surface were evaluated.

Optical microscopy. Optical microscopy was performed with a DM6 optical microscope (Leica Microsystems, Wetzlar, Germany) in transmitted light mode with 100 times magnification. For the evaluation of coalescence behavior, a THMS 600 hot stage (Linkam Scientific Instruments, Tadworth, United Kingdom) was installed. The following temperature program was used: (1) 25 – 210°C @ 50°C/min; (2) isothermal 5 min; (3) 210 – 230°C/min @ 5°C/min; (4) isothermal 10 min. An image was acquired every four seconds.

Results and Discussion

Particle size and shape

The volume-based size distribution of the starting virgin powder, measured with dynamic light scattering, is shown in figure 3. A typical SLS powder exhibits a particle size distribution that stretches from 10 to 150 µm [10]. In case of the PBT powder under investigation, 90% of the particle size by volume falls within this range. The powder has a D_{10} of 10.0 µm, a D_{50} of 41.5 µm, and a D_{90} of 100.8 µm.

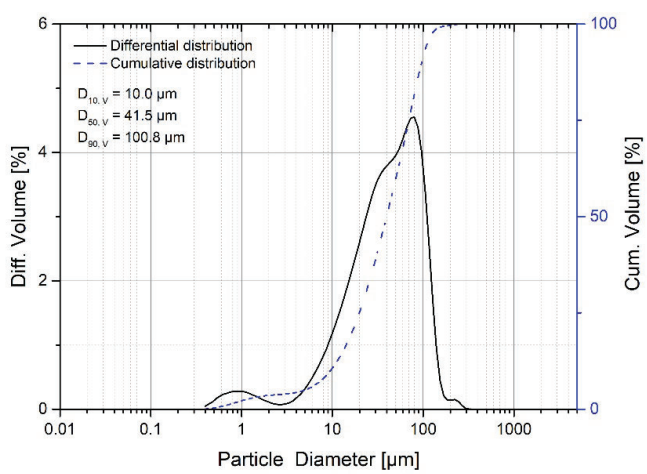

Figure 3. Differential (black, solid line) and cumulative (blue, dashed line) size distribution of the starting PBT powder.

The particle shape and morphology was qualitatively evaluated with SEM, two images are shown in figures 4 and 5. The particles have a clear spherical shape. The magnified image in figure 5 shows that the surface of the particles is smooth, no porosity neither satellites are observed. As is also indicated by the small initial peak around 1 µm in the size distribution in figure 3, there is a considerable amount of small particles, which mainly seem to be clustered around the larger particles.

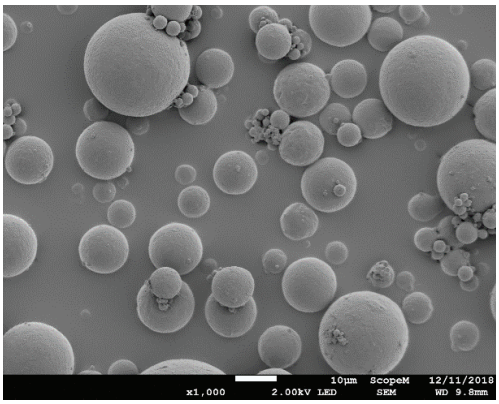

Figure 4. Overview of spherical PBT particles

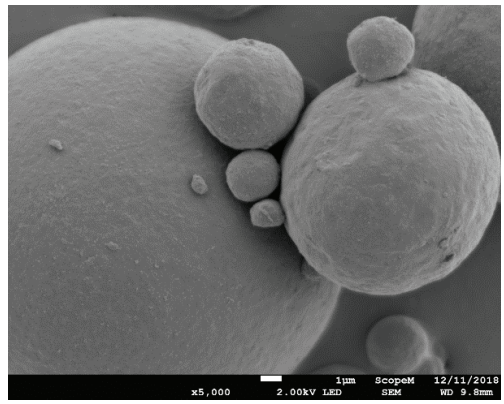

Figure 5. Detail of PBT particles

Thermal properties

The first heating and cooling DSC traces of the investigated PBT and flow aid blends are shown in figure 6. The curves have been overlaid to emphasize any differences. The melting peaks in the first heating curves overlap almost perfectly, indicating that the addition of flow aid does not have any effect on the macroscopic melting behavior. Similarly, no significant effect of the presence of flow aid on the crystallization during cooling is observed. These results correspond well with findings from Arai et al. [4], who also did not find any difference in thermal behavior between PBT powders with and without 0.1 wt.-% Aerosil®RA200H flow aid.

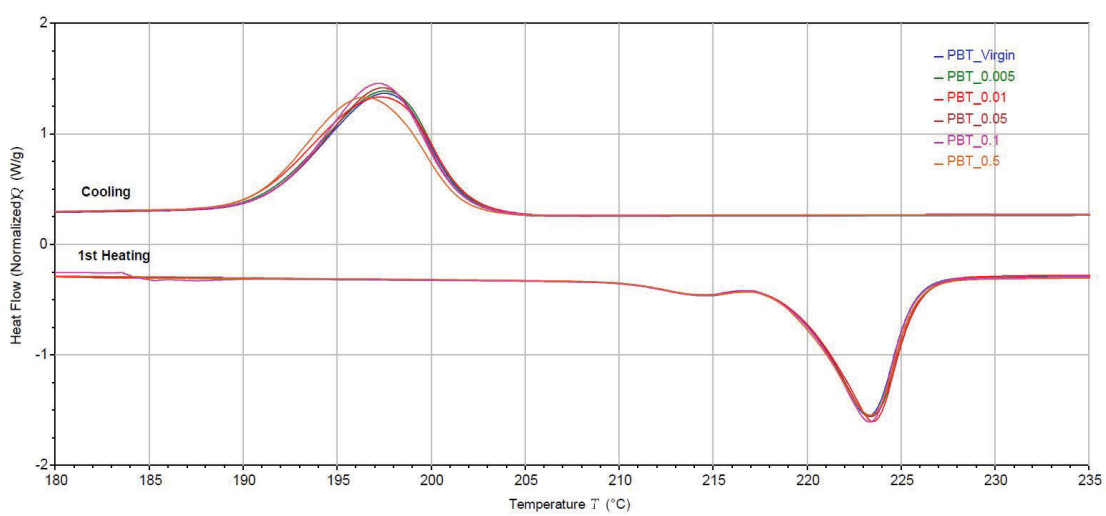

Figure 6. 1st Heating and cooling DSC traces of PBT with different amounts of flow aid.

Powder Flowability

The bulk, free-flowing density of the powder as a function of the amount of flow aid is shown in figure 7. The virgin powder with no flow aid has a low bulk density, indicative of a poorly flowing powder. Addition of 0.005 and 0.01 wt.-% flow aid does not contribute much to increasing density. When the powder contains 0.05 wt.-% flow aid however, a sharp increase of the density is observed. Flow aid concentrations above 0.05 wt.-% only slightly improve the bulk density.

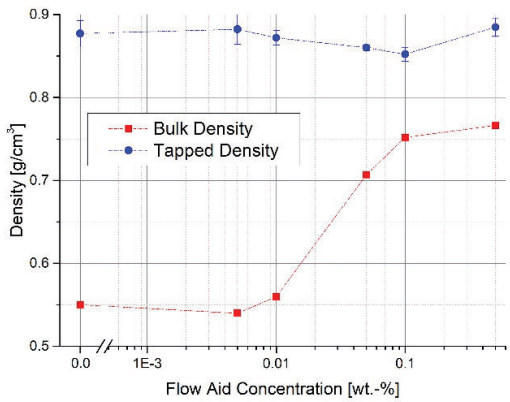

Figure 7. Powder bulk, free-flowing density for powders with different flow aid concentration. Dashed lines between data points are to guide the eye

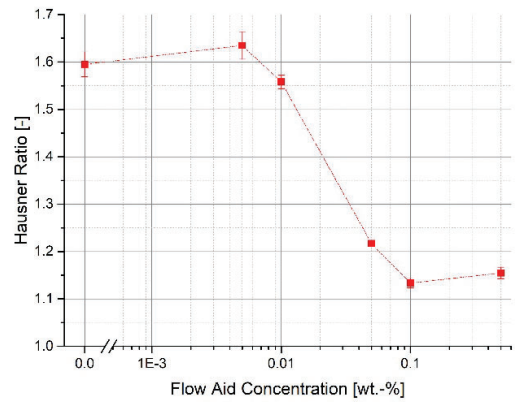

Figure 8. Hausner Ratio for powders with different flow aid concentration. Dashed lines between data points are to guide the eye

Similar behavior can be observed in the development of the Hausner ratio with different amounts of flow aid, shown in figure 8. Two plateaus of low and high flowability exist, with a narrow transition region in between. The Hausner ratio shows the same behavior as the bulk density as it combines the bulk density with the tapped density. Even though the powder with 0.05 wt.-% or more flow aid packs more densely in its free-flowing state than powder with no or low amounts of flow aid, the size and shape of the particles is the same for all powders. The tapped density depends on these two factors. After a sufficient amount of taps, the tapped density for a powder with the same size and shape of particles, is the same.

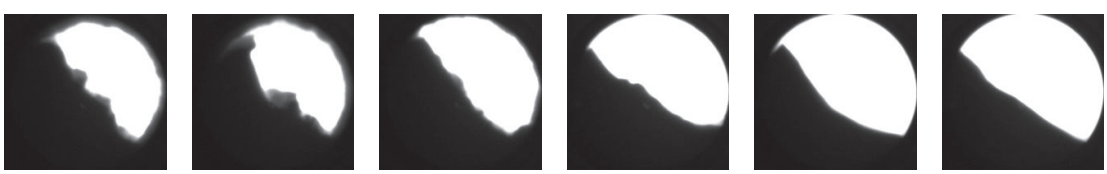

(a) PBT_Virgin **(b)** PBT_0.005 **(c)** PBT_0.01 **(d)** PBT_0.05 **(e)** PBT_0.1 **(f)** PBT_0.5

Figure 9. Snapshots of powders in the Revolution Powder Analyzer (RPA) drum.

The powder flowability was also investigated in a Revolution Powder Analyzer (RPA). The RPA consists of a rotating drum with transparent lids, through which the powder flow is evaluated with a digital camera and image recognition software. Amongst other parameters, the RPA allows for the determination of the powder avalanche angle α_A and the avalanche fractal f_A. The avalanche angle represents the resistance of the powder to flow, which strongly depends on the interparticle friction. The smoothness of the powder surface after an avalanche is expressed by the surface fractal, which is not only governed by the interparticle fraction, but also dependent on the particle size and geometry. Detailed investigations regarding powder

characteristics and respective flow properties were carried out by Amado et al. [17] and Vetterli [18].

Figure 9 shows snapshots of the powder as seen by the camera through the drum during a measurement. With increasing flow aid amount, the powder surface transitions from very irregular for blends containing 0.01 wt.-% and less flow aid (figure 9a-c), to smooth for blends containing more than 0.01 wt.-% (figure 9d-f). The powder also sticks to the surface all around the sides of the drum for blends with equal or less than 0.01 wt.-% flow aid. Visually, it is already possible to distinguish between two flow regimes; one with poor powder flowability where the flow aid concentration is 0.01 wt.-% or less, and one with better powder flowability at higher amounts of flow aid.

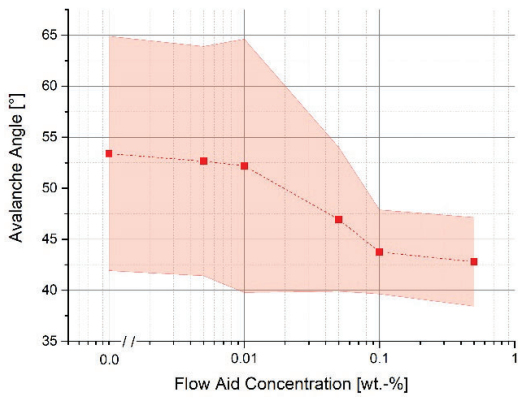

Figure 10. Average avalanche angle for powders with different flow aid concentration. Dashed lines between data points are to guide the eye. The shaded region indicates the width of the avalanche angle distribution as expressed by its standard deviation.

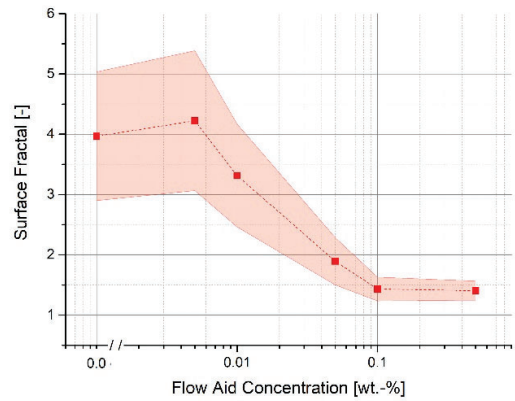

Figure 11. Average surface fractal for powders with different flow aid concentration. Dashed lines between data points are to guide the eye. The shaded region indicates the width of the surface fractal distribution as expressed by its standard deviation.

Both the avalanche angle and surface fractal, shown in figures 10 and 11 respectively, show a similar trend in dependence of flow aid concentration as the Hausner ratio. In addition to the presence of two plateaus of low and high flowability with a transition region in between, the consistency of powder flow gradually increases with increasing flow aid concentration. This is indicated by the shaded region in figures 10 and 11. The region width is equal to the standard deviation of the avalanche angle and fractal distributions. A powder flows better and more consistently when these distributions are narrow. The high avalanche angle for PBT_0.01 shows essentially the same cohesiveness, initial resistance to powder flow as PBT_Virgin without flow aid. The associated avalanche fractal however indicates that the powder surface is smoother for PBT_0.01, showing that the flow aid is mainly acting when the powder is in movement. The gradual decrease of the surface fractal standard deviation with increasing amounts of flow aid very neatly describes its effect on the powder flowability.

The existence of the two flowability plateaus and transition region can be explained by the working principle of flow aids. As discussed in the introduction, flow aids reduce friction between particles by electrostatic repulsion. There is an optimal flow aid concentration, close to the point where the particle surface is saturated. Less flow aid means the particles still rub against their own surfaces during flow, increasing friction and decreasing bulk density. More flow aid is not contributing to better flowability, because the particle surface is already saturated. This behavior is very similar to what happens with the surface tension of a liquid when a surfactant is added, until a certain critical micelle concentration is reached, described in [8,19].

Particle Coalescence

The coalescence of powder particles was tracked with HS-OM. The first column of figure 12 shows micrographs of the particles at 210°C, at the start of the measurement. Micrographs of the powders at increasing temperatures are shown in the subsequent columns. Compared to all other powders that contain flow aid, the particles of the virgin blend start to melt and coalesce at the lowest temperature.

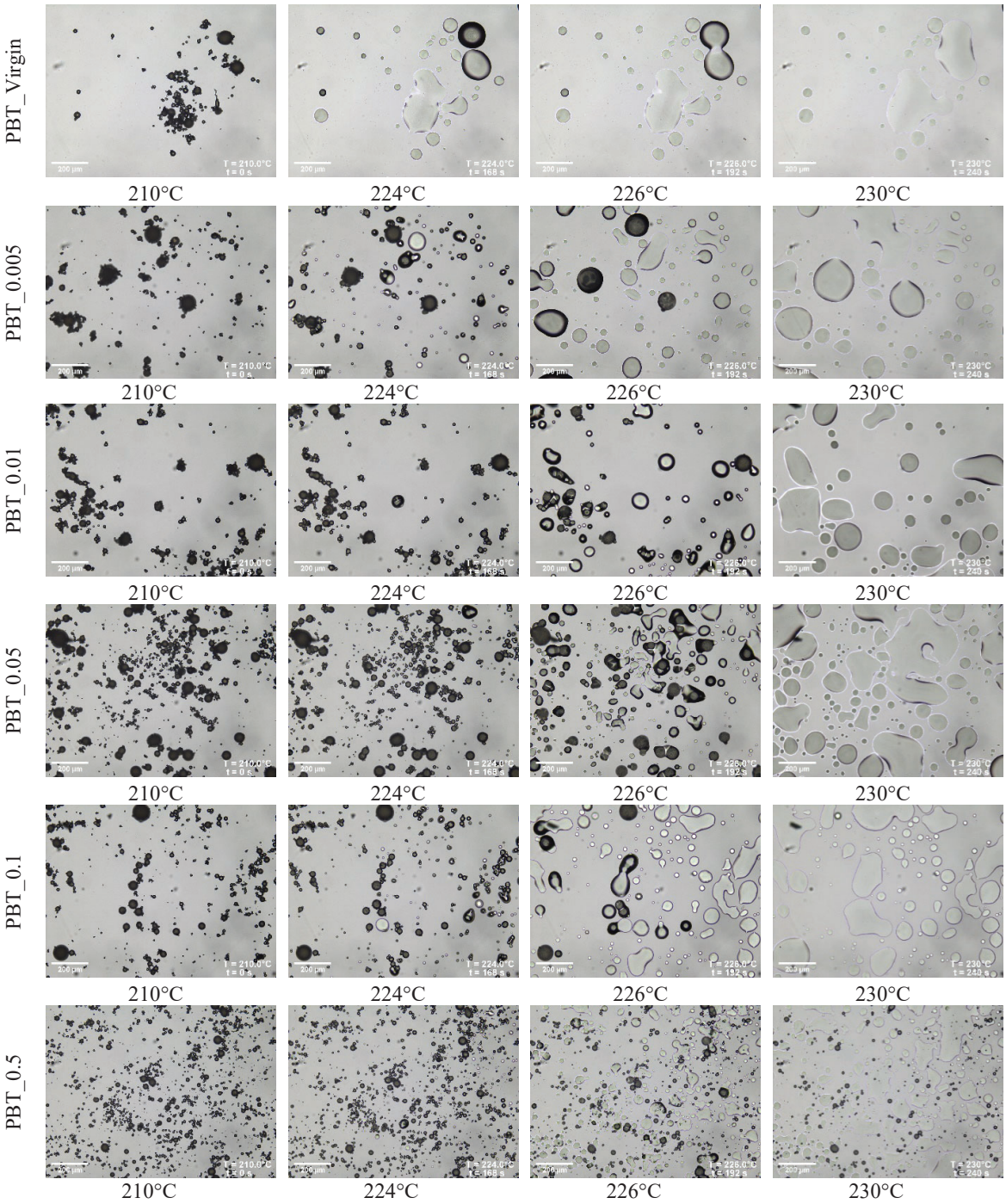

Figure 12. Micrographs of PBT powders during the hot-stage optical microscopy measurement. The scale bar in the bottom left of each micrograph is equal to 200 µm.

Already at 224°C, almost all particles have lost their spherical shape, and have completely transitioned into the molten state. At this temperature, coalescence has also progressed considerably for the PBT_0.005 powder, yet some non-molten particles remain. At increasing amounts of flow aid, smaller amounts of powder are flowing and coalescing.

The first melting curves of the DSC measurements show no effect of the flow aid on the onset of melting. This however is in contrast to the observations in HS-OM. The powders should all melt at the same temperature, but they do not seem to do so. There are two possible explanations for this effect. One reason could be differences in heat transfer to the particles. The particles are laying on a glass slide, heat is only supplied from the bottom through the slide. Since the particles are spherical, the contact area is quite small. For the smallest particles, this is no limiting factor. As can be observed, these are always the first to melt. If however a large particle with a much lower surface-to-volume ratio, is laying by itself, untouched by other, smaller particles, it can take a reasonable time before enough heat is transferred to melt it completely. Addition of flow aid separates particles from each other, which may explain why PBT_Virgin and PBT_0.005 melt relatively quickly; their particles are clustered together. Powders with higher amounts of flow aid are more dispersed, and therefore need more time and temperature to melt.

One observation that seems to contradict this explanation is the melting behavior of PBT_0.5 in the bottom row of figure 12. At 230°C, a considerable amount of non-molten particles is still present. Some of these are surrounded by polymer melt, which should facilitate heat transfer, yet they melt only after several minutes at 230°C. At this temperature, no gradual melting is observed, but the particles seem to burst and disappear almost instantaneously. In this case, the flow aid can act as a thermal insulator. In sufficient quantities, the flow aid particles form a dense network with a structure comparable to the structure of aerogels. As described in [20], aerogels have an extremely low thermal conductivity. To investigate the amount of flow aid on the surface of particles, SEM images were acquired of PBT_Virgin, PBT_0.05, and PBT_0.5. The images are shown in figure 13.

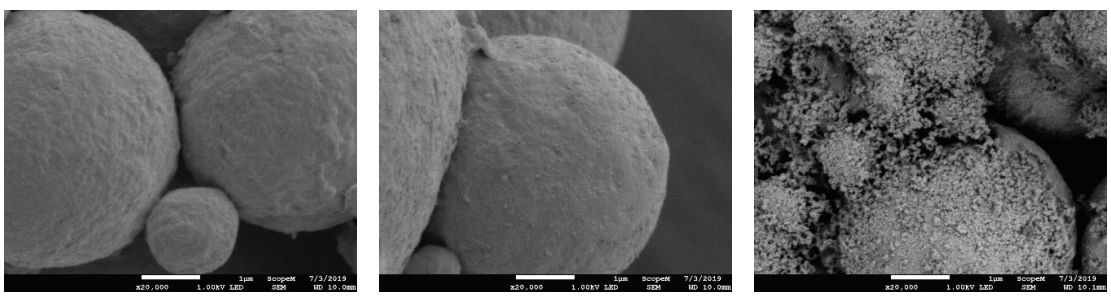

(a) **PBT_Virgin** **(b)** **PBT_0.05** **(c)** **PBT_0.5**

Figure 13. SEM images at 20’000x magnification of virgin and blended PBT powders. Length of the scale bar is equal to 1 µm

As expected, no flow aid particles are visible on the surface of PBT_Virgin particles. Upon close inspection, flow aid particles are present in PBT_0.05, but they do not saturate the surface. For PBT_0.5 however, the flow aid completely covers the surface of the particles. Additionally, the flow aid is present in the form of aggregates between the particles. This confirms the similarity of the flow aid nanopowder and an aerogel in terms of morphology.

The delayed melting is demonstrated by PBT_0.5 only. The other blends melt more gradually, even though that tends to happen at increasing temperatures with increasing flow aid concentration. In terms of powder flowability, at 0.1 and 0.5 wt.-% a plateau is reached, after

which it is unlikely to see drastic improvements. This indicates the particle surface starts to be saturated with flow aid only at these high amounts. PBT_0.1 does not exhibit delayed melting, but does show show optimal flowability in terms of Hausner ratio, avalanche angle, and avalanche fractal. The optimal flow aid concentration likely lies around this point.

Conclusions and Outlook

The effect of different amounts of flow aid on the flowability and coalescence of a PBT polymer powder consisting of spherical particles was determined. The flowability as a function of flow aid concentration can be divided into three regions; the first consists of a plateau of low flowability where there is no measurable effect of flow aid addition, up to amounts of approximately 0.01 wt.-%. This is followed by a sharp transition region over the range between 0.01 and 0.05 wt.-% after which another plateau region of high flowability for concentrations higher than 0.1 wt.-% is reached. Addition of even the smallest amount of flow aid shifts the the coalescence of particles to a higher temperature by approximately 2°C. With increasing amounts of flow aid, coalescence is delayed further. A special case occurs for PBT with 0.5 wt.-% flow aid. Some particles remain solid at high temperatures, disappearing almost instantaneously after a few minutes. Both the flowability and melting behaviors show analogies with surfactant behavior. Mechanisms that hold for surfactants may therefore be applied to systems containing flow aids, which can be helpful to determine the optimal amount of flow aid to add to a powder.

The current work summarized the results from initial investigations into powder flow and coalescence behavior as a function of flow aid concentration. There are multiple possibilities to extend the study to gain a better understanding of the interplay between powders and flow aids. An obvious start is to investigate the effect of flow aids with different chemistry. The Aerosil ® R 812 used in this study is a general-purpose hydrophobic flow aid, but there are many other variants that are likely to have a different influence on powder coalescence and flow. To increase the resolution and validity of the results of the current study, it is necessary to investigate additional blends with different flow aid concentrations. The most interesting blends lie in the flowability transition region between 0.01 and 0.05 wt.

Although it is possible to distinguish the differences in flowing behavior of powders containing different amounts of flow aid visually, quantification based on the current results is difficult. The particle size is related to the observed melting temperature. That also means that in order to evaluate the results properly, only particles with similar size should be considered. This was not possible with the current measurements, but it is possible to track the coalescence of two similar particles at higher magnification, similar to the method of Berretta et al. [12]. These measurements can also be done at lower heating rates such as 0.5°C/min. Coalescence then occurs quasi-isothermally, and can be related to existing models for the coalescence of two viscoelastic particles. In this way, the dominating effects can be determined and help to explain the observed behavior.

Finally, it is important to establish the link between the results measured in the laboratory and the performance of the powder in the SLS process. This was not possible in the current study due to the limited amount of available material. Solutions that allow for the evaluation of part density also for small amounts of powder are currently being developed, and will be used in further research.

Acknowledgements

Luiz Morales of the Scientific Center for Optical and Electron Microscopy (ScopeM) at ETH Zürich is acknowledged for his assistance with acquiring SEM images.

References

1. Schmid, M.; Kleijnen, R.; Vetterli, M.; Wegener, K. Influence of the origin of polyamide 12 powder on the laser sintering process and laser sintered parts. *Appl. Sci.* **2017**, *7*, DOI: 10.3390/app7050462.
2. Lexow, M.M.; Drummer, D. New Materials for SLS: The Use of Antistatic and Flow Agents. *J. Powder Technol.* **2016**, *2016*, 1–9, DOI: 10.1155/2016/4101089.
3. Laumer, T.; Stichel, T.; Raths, M.; Schmidt, M. Analysis of the influence of different flowability on part characteristics regarding the simultaneous laser beam melting of polymers. *Phys. Procedia* **2016**, *83*, 937–946, DOI: 10.1016/j.phpro.2016.08.098.
4. Arai, S.; Tsunoda, S.; Kawamura, R.; Kuboyama, K.; Ougizawa, T. Comparison of crystallization characteristics and mechanical properties of poly(butylene terephthalate) processed by laser sintering and injection molding. *Mater. Des.* **2017**, *113*, 214–222, DOI: 10.1016/j.matdes.2016.10.028.
5. Rietzel, D. Werkstoffverhalten und Prozessanalyse beim Laser-Sintern von Thermoplasten. **2011**, 130.
6. Berretta, S.; Ghita, O.; Evans, K.E. Morphology of polymeric powders in Laser Sintering (LS): From Polyamide to new PEEK powders. *Eur. Polym. J.* **2014**, *59*, 218–229, DOI: 10.1016/j.eurpolymj.2014.08.004.
7. Blümel, C.; Schmidt, M.; Peukert, W.; Winzer, B.; Laumer, T.; Schmidt, J.; Sachs, M.; Wirth, K.-E. Increasing flowability and bulk density of PE-HD powders by a dry particle coating process and impact on LBM processes. *Rapid Prototyp. J.* **2015**, *21*, 697–704, DOI: 10.1108/rpj-07-2013-0074.
8. Evonik Industries *AEROSIL ® - Fumed Silica Technical Overview*;
9. Rumpf, H. Die Wissenschaft des Agglomerierens. *Chemie Ing. Tech.* **1974**, *1*, 1–46.
10. Schmid, M. *Laser Sintering with Plastics*; Hanser Verlag, 2018;
11. Benedetti, L.; Brulé, B.; Decraemer, N.; Evans, K.E.; Ghita, O. Evaluation of particle coalescence and its implications in laser sintering. *Powder Technol.* **2019**, *342*, 917–928, DOI: 10.1016/j.powtec.2018.10.053.
12. Berretta, S.; Wang, Y.; Davies, R.; Ghita, O.R. Polymer viscosity, particle coalescence and mechanical performance in high-temperature laser sintering. *J. Mater. Sci.* **2016**, *51*, 4778–4794, DOI: 10.1007/s10853-016-9761-6.
13. Verbelen, L.; Dadbakhsh, S.; Eynde, M. Van Den; Kruth, J.; Goderis, B.; Puyvelde, P. Van Characterization of polyamide powders for determination of laser sintering processability. *Eur. Polym. J.* **2016**, *75*, 163–174, DOI: 10.1016/j.eurpolymj.2015.12.014.
14. Dadbakhsh, S.; Verbelen, L.; Verkinderen, O.; Strobbe, D.; Puyvelde, P. Van; Kruth, J. Effect of PA12 powder reuse on coalescence behaviour and microstructure of SLS parts. *Eur. Polym. J.* **2017**, DOI: 10.1016/j.eurpolymj.2017.05.014.
15. Hejmady, P.; Breemen, C.A. Van; Anderson, P.D. Soft Matter Laser sintering of polymer particle pairs studied by in situ visualization †. **2019**, DOI: 10.1039/c8sm02081g.
16. Kleijnen, R.G.; Schmid, M.; Wegener, K. Production and Processing of a Spherical Polybutylene Terephthalate Powder for Laser Sintering. *Appl. Sci.* **2019**, *9*, 1308, DOI: 10.3390/app9071308.
17. Amado, A.; Schmid, M.; Levy, G.; Wegener, K. Advances in SLS Powder Characterization. In Proceedings of the Proceedings of the Direct Digital Manufacturing

Conference; Berlin, 2012; pp. 438–452.
18. Vetterli, M. Powder Optimization for Laser Sintering - An insight in powder intrinsic and extrinsic properties, ETH Zurich, 2019.
19. Butt, H.-J.; Graf, K.; Kappl, M. *Physics and Chemistry of Interfaces*; Wiley-VCH: Weinheim, 2006; ISBN 978-3-527-40629-6.
20. Hrubesh, L.W.; Pekala, R.W. Thermal properties of organic and inorganic aerogels. *J. Mater. Res.* **1994**, *9*, 731–738, DOI: 10.1557/jmr.1994.0731.